International Journal of Bifurcation and Chaos, Vol. 30, No. 14 (2020) 2030042 (14 pages)

DOI: 10.1142/S0218127420300426

Hidden Attractors with Conditional Symmetry

Chunbiao Li* and Jiayu Sun†
Jiangsu Collaborative Innovation Center of Atmospheric Environment and Equipment Technology (CICAEET), Nanjing University of Information Science and Technology, Nanjing 210044, P. R. China
School of Artificial Intelligence Nanjing University of Information Science and Technology, Nanjing 210044, P. R. China
Collaborative Innovation Center of Memristive Computing Application (CICMCA), Qilu Institute of Technology, Jinan 250200, P. R. China
*goontry@126.com
*chunbiaolee@nuist.edu.cn
†sunjy9512@163.com

Julien Clinton Sprott
Department of Physics, University of Wisconsin–Madison, Madison, WI 53706, USA
sprott@physics.wisc.edu

Tengfei Lei
Collaborative Innovation Center of Memristive Computing Application (CICMCA), Qilu Institute of Technology, Jinan 250200, P. R. China
leitengfeicanhe@126.com

Received January 19, 2020; Revised April 16, 2020

By introducing an absolute value function for polarity balance, some new examples of chaotic systems with conditional symmetry are constructed that have hidden attractors. Coexisting oscillations along with bifurcations are investigated by numerical simulation and circuit implementation. Such new cases enrich the gallery of hidden chaotic attractors of conditional symmetry that are potentially useful in engineering technology.

Keywords: Hidden attractor; offset boosting; conditional symmetry; bifurcation; chaos.

*Author for correspondence

1. Introduction

Hidden oscillation has evoked great attention for its potential threat to engineering applications, especially for chaotic systems which are especially problematic. Finding various hidden chaotic attractors in dynamical systems has become a popular topic in studies of nonlinear dynamical systems. The Chua system [Leonov & Kuznetsov, 2013; Leonov *et al.*, 2011, 2012, 2015; Zhang & Wang, 2019; Bao *et al.*, 2016], Lorenz or Lorenz-like systems [Li & Sprott, 2014a; Bao *et al.*, 2017a], and those chaotic flows with stable equilibria [Molaie *et al.*, 2013; Sprott, 2014], line equilibria [Li *et al.*, 2014; Jafari & Sprott, 2013a; Bao *et al.*, 2017b], or no equilibria [Li *et al.*, 2016b; Jafari & Sprott, 2013b; Sprott, 2015] can exhibit chaos, which is hidden since it cannot be found using an initial condition in the neighborhood of an equilibrium point. Therefore, much more effort has been made to find hidden chaotic [Yang *et al.*, 2010; Wang & Chen, 2012; Jafari *et al.*, 2016; Jesus *et al.*, 2018; Nazarimehr *et al.*, 2018; Pham *et al.*, 2017; Pham *et al.*, 2018; Tang *et al.*, 2018; Bayani *et al.*, 2019; Çavuşoğlu *et al.*, 2019] or hyperchaotic attractors [Wei *et al.*, 2015; Pham *et al.*, 2015; Zhou *et al.*, 2018a]. Hidden attractors and stable equilibrium points are two independent types of stability characterizing the long-time evolution of a dynamical system. In particular, hidden chaos or hyperchaos are not associated with any equilibria.

Furthermore, the structure of a dynamical system can show this independence. Symmetric systems even with different kinds of equilibria exhibit coexisting symmetric pairs of chaotic attractors when the symmetry is broken [Sprott, 2014; Zhou *et al.*, 2018b; Wang *et al.*, 2014; Li *et al.*, 2015a; Li *et al.*, 2015b; Li *et al.*, 2015c]. Asymmetric systems can also produce coexisting strange attractors of conditional symmetry when an additionally introduced function maintains the polarity balance [Li *et al.*, 2017; Li *et al.*, 2018; Li *et al.*, 2019; Li & Sprott, 2017; Li *et al.*, 2016a]. In fact, hidden oscillation, equilibria, and system structure may combine to give abundant possibilities for the generation of chaos. Conditional symmetric chaos as a new class of hidden attractor has not been reported, supplementing those chaotic systems with no equilibria or with a line of equilibrium points. Exploring such cases of conditional symmetry can help us understand the mechanism of attractor doubling and polarity transformation. In this paper, several new examples of chaotic systems with conditional symmetry are proposed in Sec. 2. Such systems are said to have hidden attractors of conditional symmetry when the chaotic flows occur in the absence of equilibria or with lines of equilibria. In Sec. 3, the basic dynamics of these systems are described including coexisting bifurcations by numerical simulation. In Sec. 4, the corresponding circuit implementation provides experimental proof. Some extended discussion and conclusion are in the last section.

2. New Chaotic Attractors of Conditional Symmetry

For a dynamical system $\dot{X} = F(X)$ ($X = (x_1, x_2, \ldots, x_N)^T$), if there exists a variable substitution including polarity reversal and offset boosting such as $u_{i_1} = -x_{i_1}$, $u_{i_2} = -x_{i_2}, \ldots, u_{i_k} = -x_{i_k}$, $u_{j_1} = x_{j_1} + d_{j_1}, u_{j_2} = x_{j_2} + d_{j_2}, \ldots, u_{j_l} = x_{j_l} + d_{j_l}$, $u_i = x_i$, (here $1 \leq i_1, \ldots, i_k \leq N, 1 \leq j_1, \ldots, j_l \leq N, i_1, \ldots, i_k$ and $j_1, \ldots, j_l$ are not identical, $i \in \{1, 2, \ldots, N\} \backslash \{i_1, \ldots, i_k, j_1, \ldots, j_l\}$), the derived system retains its balance of polarity on the two sides of the equation and will satisfy $\dot{U} = F(U)$ ($U = (u_1, u_2, \ldots, u_N)$), then the system $\dot{X} = F(X)$ has l-dimensional conditional symmetry since the polarity balance depends on an l-dimensional offset boosting [Li *et al.*, 2018]. Applying a suitable absolute value function in those reported chaotic systems with a hidden attractor to realize offset-boosting-based polarity balance, several new examples of hidden attractors with conditional symmetry can be constructed. Specifically, hidden chaotic attractors have been found in chaotic systems with no equilibrium points as listed in Table 1. In this work, for obtaining representative Lyapunov exponents rather than absolute ones [Leonov *et al.*, 2015; Kuznetsov *et al.*, 2018; Kuznetsov & Mokaev, 2019], all the finite-time LEs are computed for the time interval $[0, 10^6]$ for the initial points on the attractor using Wolf's algorithm [Wolf *et al.*, 1985]. The table also shows their revised versions with conditional symmetry, all of which share the following properties:

(a) All of the conditional symmetric cases are of conditional rotational symmetry;
(b) All the original cases and conditional symmetric cases share almost the same Lyapunov exponents and Kaplan–Yorke dimensions;
(c) All the conditional symmetric versions derive their polarity balance from offset boosting in the z dimension;

Table 1. Chaotic Systems with No Equilibria (CSNE) and their Conditional Symmetric versions (CSNECS).

Systems	Equations	Parameters	LEs	D_{KY}	(x_0, y_0, z_0)
CSNE1	$\dot{x} = -y$, $\dot{y} = x + z$, $\dot{z} = 2y^2 + xz - a$	$a = 0.35$	0.0776, 0, -1.5008	2.0517	0, 0.4, 1
CSNECS1	$\dot{x} = -y$, $\dot{y} = x + F(z)$, $\dot{z} = 2y^2 + xF(z) - a$, $F(z) = \|z\| - 5$	$a = 0.35$	0.0776, 0, -1.5008	2.0517	0, 0.4, 6 0, 0.4, -5
CSNE2	$\dot{x} = y$, $\dot{y} = -x + z$, $\dot{z} = -0.8x^2 + z^2 + a$	$a = 2.0$	0.0252, 0, -6.8521	2.0037	0, 2.3, 0
CSNECS2	$\dot{x} = y$, $\dot{y} = -x + F(z)$, $\dot{z} = -0.8x^2 + F(z)^2 + a$, $F(z) = \|z\| - 12$	$a = 2.0$	0.0252, 0, -6.8521	2.0037	0, 2.3, 12 0, -2.3, -12
CSNE3	$\dot{x} = z$, $\dot{y} = x - y$, $\dot{z} = -4x^2 + 8xy + yz + a$	$a = 0.1$	0.0654, 0, -2.0398	2.0321	0.5, 0, -1
CSNECS3	$\dot{x} = F(z)$, $\dot{y} = x - y$, $\dot{z} = -4x^2 + 8xy + yF(z) + a$, $F(z) = \|z\| - 12$	$a = 0.1$	0.0665, 0, -2.0410	2.0326	0.5, 0, 11 0.5, 0, -13
CSNE4	$\dot{x} = -y$, $\dot{y} = x + z$, $\dot{z} = xy + xz + 0.2yz - a$	$a = 0.4$	0.1028, 0, -2.1282	2.0483	2.5, 0, 0
CSNECS4	$\dot{x} = -y$, $\dot{y} = x + F(z)$, $\dot{z} = xy + xF(z) + 0.2yF(z) - a$, $F(z) = \|z\| - 15$	$a = 0.4$	0.1026, 0, -2.1275	2.0482	2.5, 0, 15 -2.5, 0, -15
CSNE5	$\dot{x} = y$, $\dot{y} = z$, $\dot{z} = x^2 - y^2 + 2xz + yz + a$	$a = 1.0$	0.0532, 0, -11.8580	2.0045	1, 0, -4
CSNECS5	$\dot{x} = y$, $\dot{y} = F(z)$, $\dot{z} = x^2 - y^2 + 2xF(z) + yF(z)$, $F(z) = \|z\| - 15$	$a = 1.0$	0.0538, 0, -11.8591	2.0045	1, 0, 11 1, 0, -19
CSNE6	$\dot{x} = y$, $\dot{y} = z$, $\dot{z} = x^2 - y^2 + xy + 0.4xz + a$	$a = 1.0$	0.1101, 0, -1.3879	2.0793	0, 1, -4.9
CSNECS6	$\dot{x} = y$, $\dot{y} = F(z)$, $\dot{z} = x^2 - y^2 + xy + 0.4xF(z) + a$, $F(z) = \|z\| - 30$	$a = 1.0$	0.1105, 0, -1.3882	2.0796	0, 1, 26.1 0, 1, -32.9

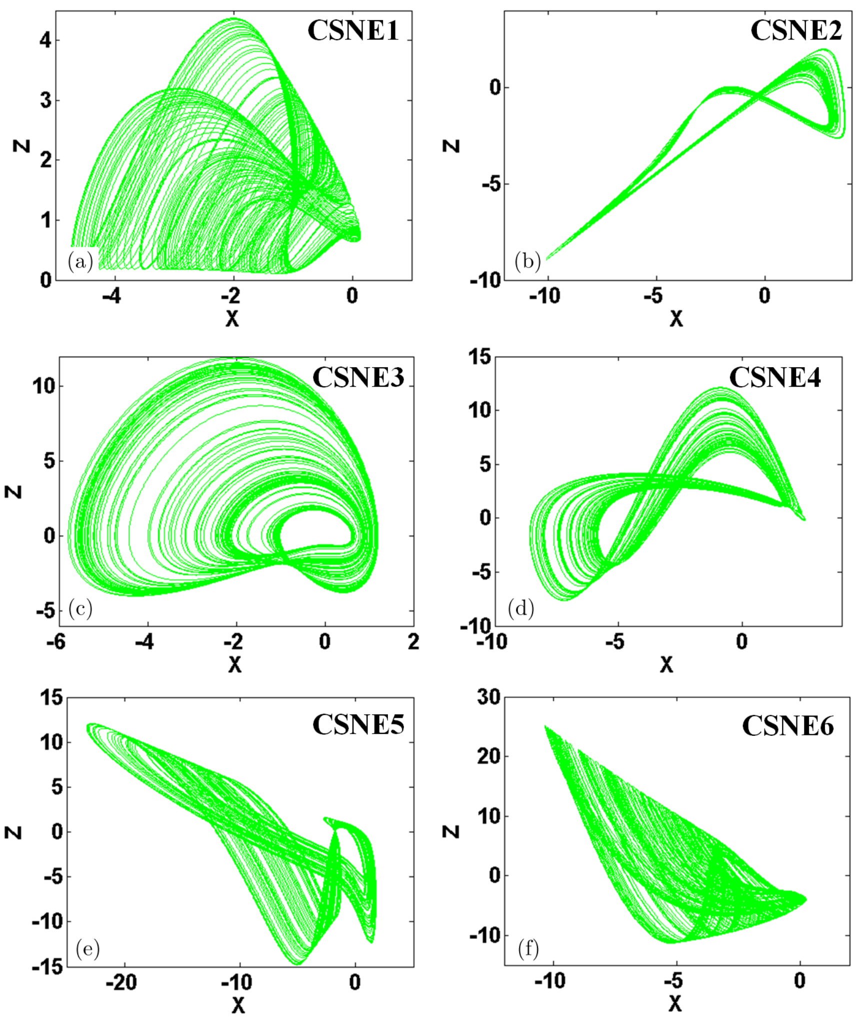

Fig. 1. Strange attractors in the original chaotic systems with no equilibria.

(d) All the conditional symmetry results from 1D offset boosting.

The strange attractors and their conditional symmetric versions are shown in Figs. 1 and 2, respectively. The corresponding basins of attraction for two of the conditional symmetric attractors in the plane $y = 0$ with the condition of offset-boosting in the corresponding z dimension are given in Fig. 3. While the attractors have an evident symmetry, their basins are highly asymmetric.

Table 2 lists some hidden chaotic attractors with line equilibria and their conditional symmetric versions. The conditional symmetric variants are

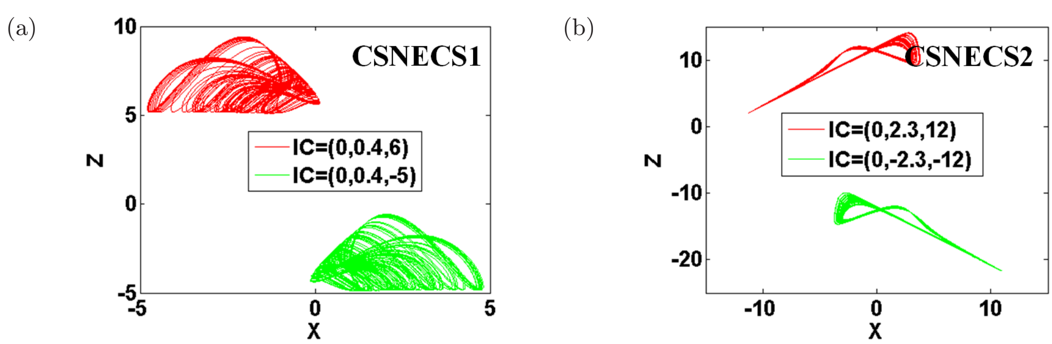

Fig. 2. Coexisting attractors of conditional rotational symmetry induced by 1D offset boosting in the z dimension.

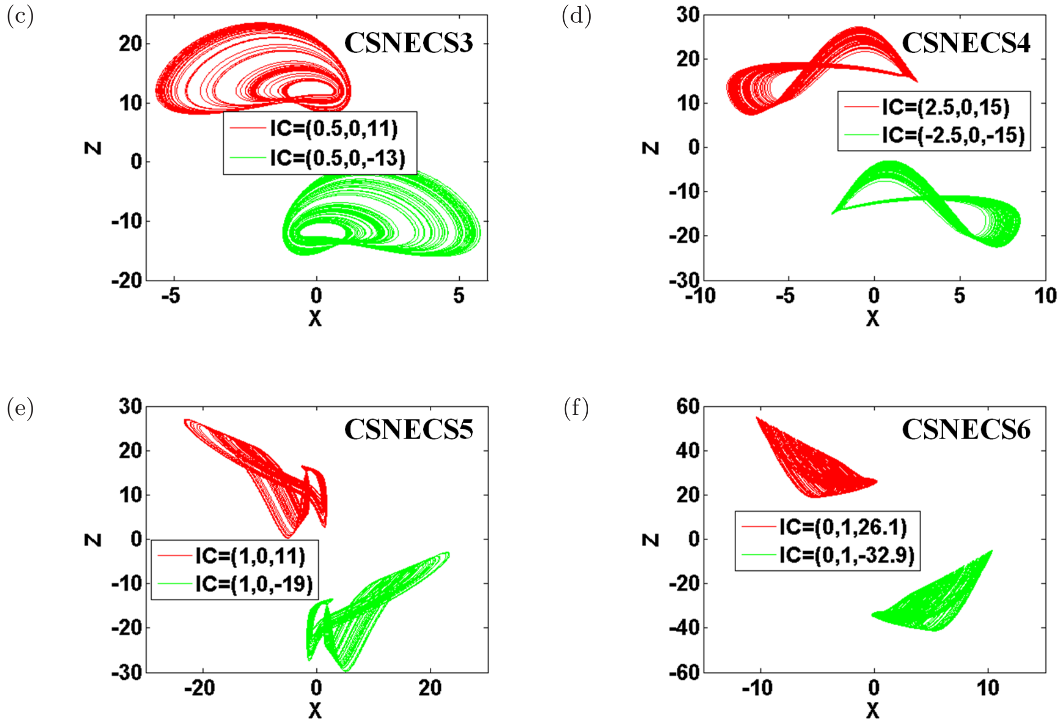

Fig. 2. (*Continued*)

obtained from 1D or 2D offset boosting in the x, z, or y and z dimensions. Figure 4. shows the original attractors, and Figs. 5–7 show the pair of hidden attractors for conditional symmetry. For the existence of a line of equilibria, all the initial conditions close to the equilibria show their power to drive the system to its line equilibria, which makes the basins of attraction fragile. The basins of attraction show the lack of symmetry as for the previous cases without any equilibria.

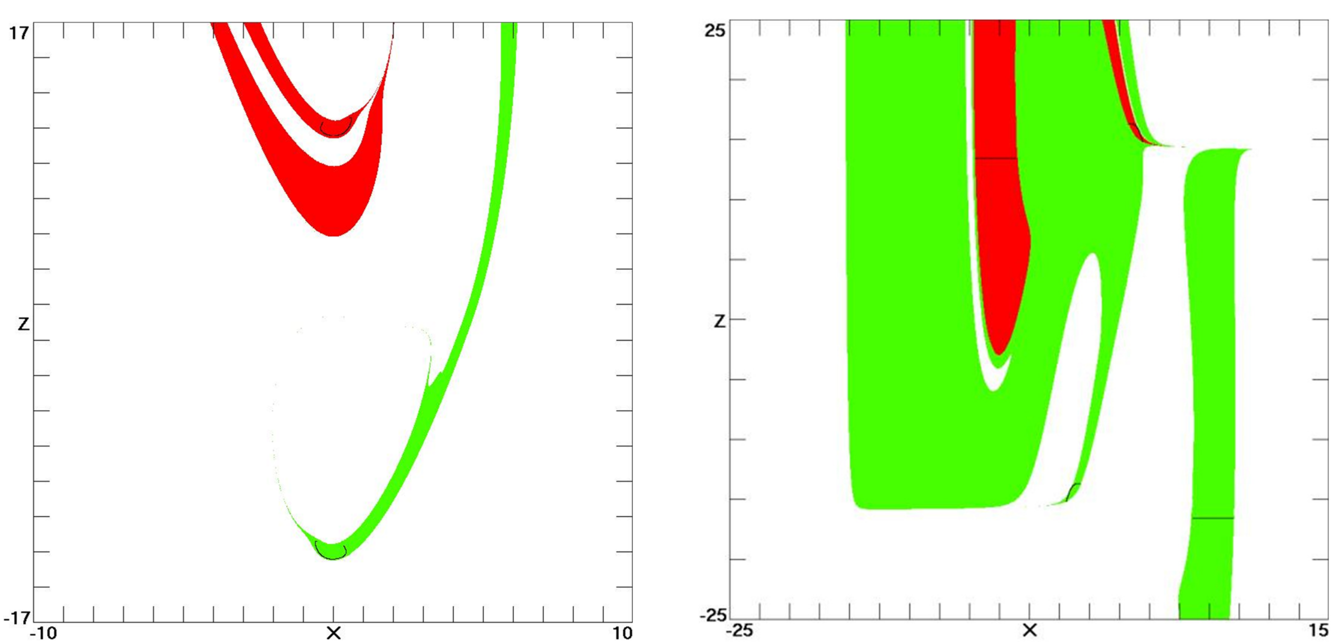

Fig. 3. Basins of attraction on $y = 0$: (a) CSNECS3 and (b) CSNECS4.

Table 2. Chaotic Systems with Line Equilibria (CSLE) and their Conditional Symmetric versions (CSLECS).

Systems	Equations	Parameters	Equilibria	Eigenvalues	LEs	D_{KY}	(x_0, y_0, z_0)
CSLE1	$\dot{x} = z,$	$a = 1.62,$	$(x, 0, 0)$	$0,$	$0.0642,$	2.0939	0, 1, 0.8
	$\dot{y} = -ay - xz,$	$b = 0.2$		$\frac{-0.62 \pm \sqrt{6.8644 - 4x^2}}{2}$	$0,$		
	$\dot{z} = z - bz^2 + xy$			-0.6842			
CSLECS1	$\dot{x} = z,$	$a = 1.62,$	$(x, 0, 0)$	$0,$	$0.0645,$	2.0943	9, 1, 0.8
	$\dot{y} = -ay - zF(x),$	$b = 0.2$		$-0.31 \pm \sqrt{-(\lvert x\rvert - 7.69)(\lvert x\rvert - 10.31)}$	$0,$		−9, 1, 0.8
	$\dot{z} = z - bz^2 + yF(x),$				-0.6845		
	$F(x) = \lvert x\rvert - 9$						
CSLE2	$\dot{x} = y,$	$a = 0.4,$	$(0, 0, z)$	0	$0.0749,$	2.1014	0, 4, 5
	$\dot{y} = ay^2 - xz,$	$b = 1$		$\pm\sqrt{-z}$	$0,$		
	$\dot{z} = x^2 + xy - bxz$				-0.7391		
CSLECS2	$\dot{x} = G(y),$	$a = 0.4,$	$(0, \pm 10, z)$	$0, \pm\sqrt{12 - \lvert z\rvert}$	$0.0749,$	2.1013	0, 14, 17
	$\dot{y} = aG(y)^2 - xF(z),$	$b = 1$		$0, \pm\sqrt{\lvert z\rvert - 12}$	$0,$		0, −6, −7
	$\dot{z} = x^2 + xG(y) - bxF(z),$				-0.7390		
	$G(y) = \lvert y\rvert - 10,$						
	$F(z) = \lvert z\rvert - 12$						
CSLE3	$\dot{x} = y,$	$a = 0.8,$	$(0, 0, z)$	$0, \pm i$	$0.0179,$	2.0437	1, 0.5, 2
	$\dot{y} = cz\lvert y\rvert + 0.1y\lvert y\rvert - x,$	$b = 0.5$			$0,$		
	$\dot{z} = 0.5x^2 - axy - bxz$	$c = 0.5$			-0.4094		
CSLECS3	$\dot{x} = y,$	$a = 0.8,$	$(0, 0, z)$	$0, \pm i$	$0.0177,$	2.0433	1, 0.5, 5
	$\dot{y} = c\lvert y\rvert F(z) + 0.1y\lvert y\rvert - x,$	$b = 0.5$			$0,$		−1, −0.5, −4
	$\dot{z} = 0.5x^2 - axy - bxF(z),$	$c = 0.5$			-0.4092		
	$F(z) = \lvert z\rvert - 4$						

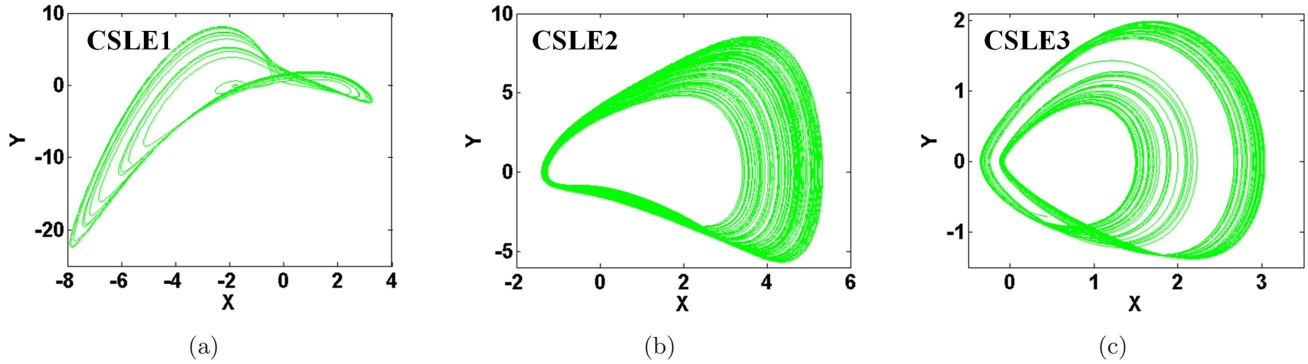

Fig. 4. Strange attractors of the original systems with line equilibria.

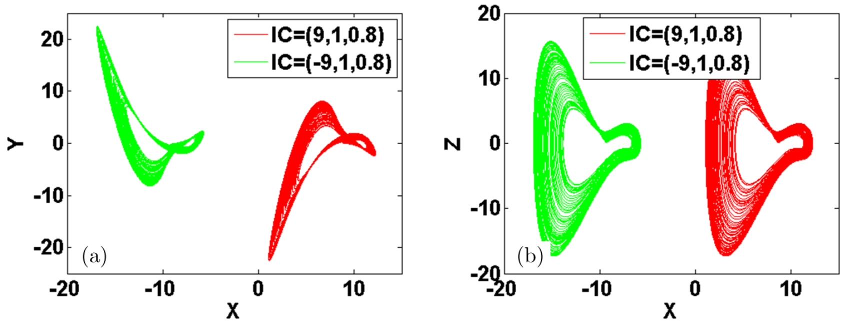

Fig. 5. Coexisting attractors in conditional symmetric system CSLECS1 induced by 1D offset boosting in the x dimension.

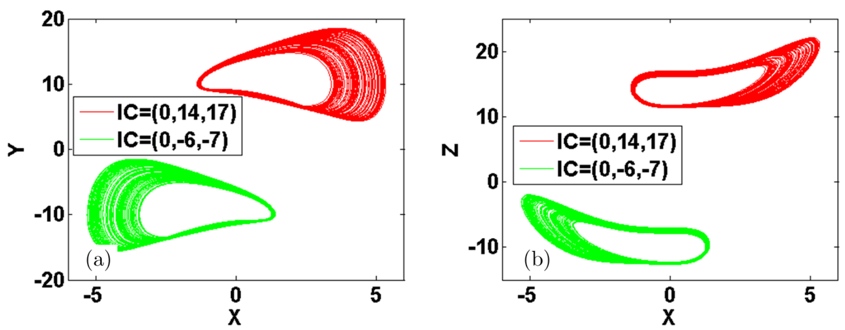

Fig. 6. Coexisting attractors in conditional symmetric system CSLECS2 induced by 2D offset boosting in the y and z dimensions.

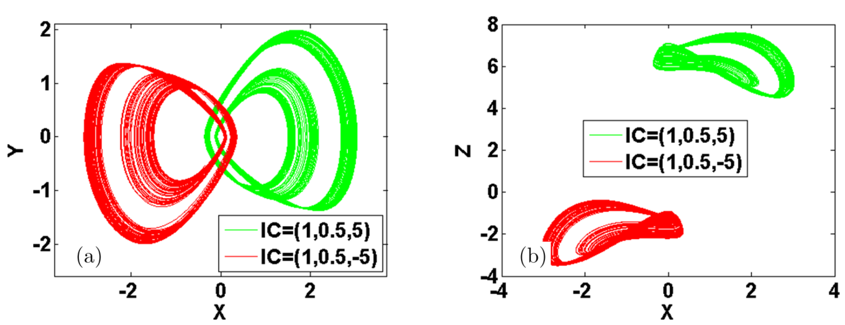

Fig. 7. Coexisting attractors in conditional symmetric system CSLECS3 induced by 1D offset boosting in the z dimension.

3. Bifurcations of Conditional Symmetry

There are two coexisting bifurcations of conditional symmetry in these new cases. As shown in Fig. 8, system CSNECS6 exhibits two separate typical period-doubling bifurcations in the corresponding basins of attraction. Typical periodic and chaotic oscillations of conditional symmetry are all exhibited. In system CSLECS3, inverse period-doubling bifurcations coexist when the parameter a varies in [0.6, 2], as shown in Fig. 9. Other bifurcations show the same property of conditional symmetry, which indicates that the corresponding system exhibits a similar dynamical evolution but in different regions of phase spaces. For example, in systems CSNECS6 and CSLECS3, one bifurcation is with

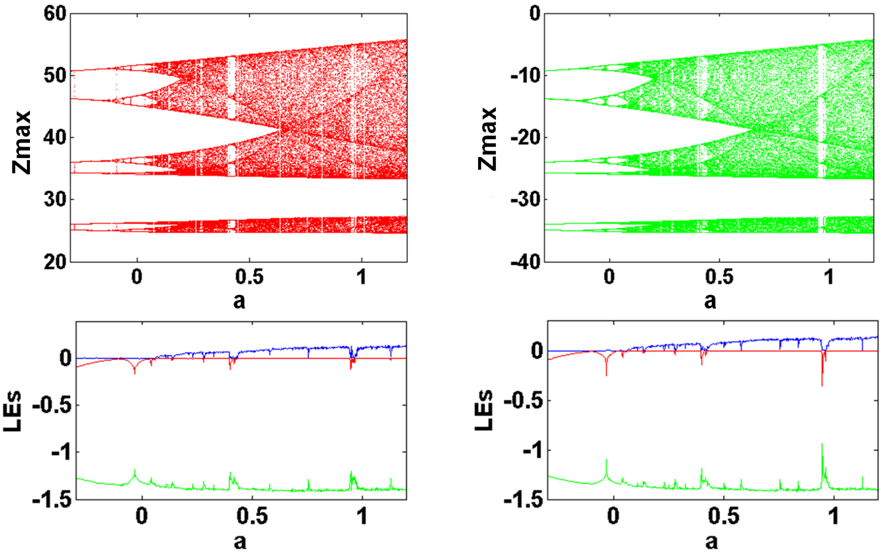

Fig. 8. Bifurcations and Lyapunov exponent spectrum in CSNECS6 when a varies in $[-0.3,\ 1.2]$. (a) IC $= (0, 1, 26.1)$ and (b) IC $= (0, 1, -32.9)$.

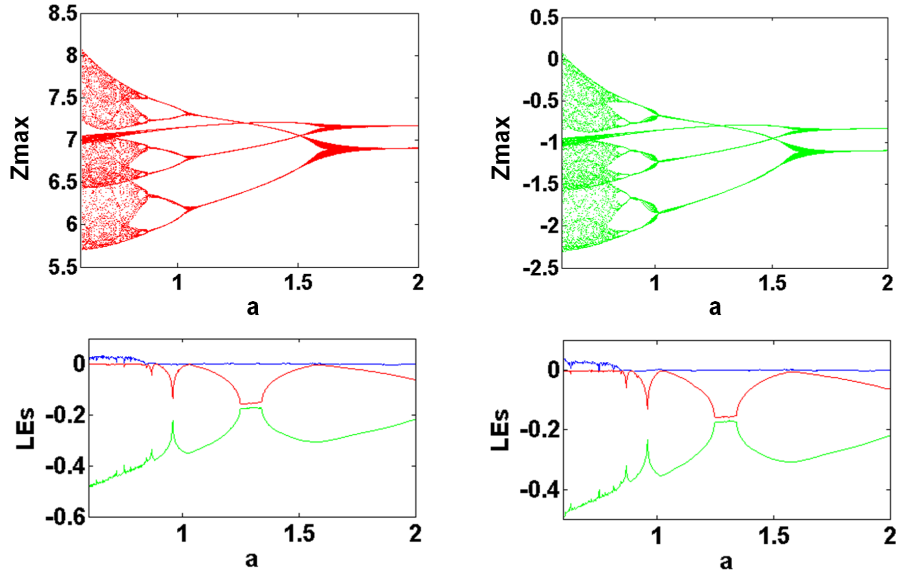

Fig. 9. Bifurcations and Lyapunov exponent spectrum in CSLECS3 with $b = 0.5$, $c = 0.5$ when a varies in [0.6, 2]: (a) IC $= (1, 0.5, 5)$ and (b) IC $= (-1, -0.5, -4)$.

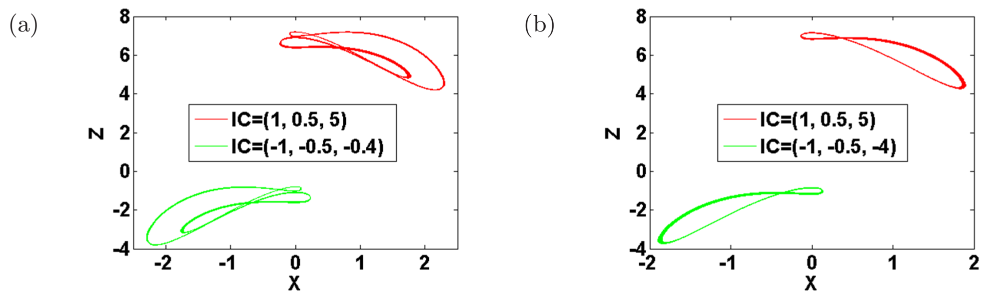

Fig. 10. Limit cycles of conditional symmetry in CSLECS3 with $b = 0.5$ and $c = 0.5$: (a) $a = 1.3$ and (b) $a = 1.7$.

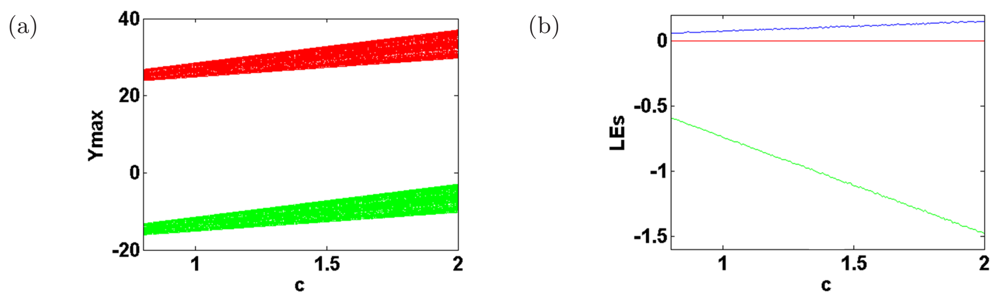

Fig. 11. Amplitude and frequency rescaling in CSLECS2 with $a = 0.4$, $b = 1$, $G(y) = |y| - 20$, $F(z) = |z| - 20$: (a) bifurcation diagram and (b) Lyapunov exponents.

negative values of z while the other is for positive values. The reason is that CSNECS6 and CSLECS3 have conditional rotational symmetry according to x and y.

All the coexisting attractors with conditional symmetry are asymmetric and undergo their own evolution separately. In CSLECS3, when $b = 0.5$ and $c = 0.5$, two pairs of coexisting limit cycles are obtained at $a = 1.3$ and $a = 1.7$, as shown in Fig. 10. System CSLE2 shares a differential equation with only a single nonquadratic term y, which provides a single knob for amplitude-frequency control [Li & Sprott, 2014b]. In system CSLE2, an additional parameter c in the first dimension can realize simultaneous amplitude and frequency control since a transformation $x \to x/c$, $y \to y/c$, $z \to z/c$, $t \to ct$ leaves an independent parameter c in the system. Correspondingly, in system CSLECS2, parameter c in Eq. (1) modifies the amplitude

$$\begin{cases} \dot{x} = cG(y), \\ \dot{y} = aG(y)^2 - xF(z), \\ \dot{z} = x^2 + xG(y) - bxF(z) \end{cases} \tag{1}$$

and frequency of producing coexisting attractors with conditional symmetry. However, this control should be limited in a certain region since the conditional symmetry depends on the attractor size. To enlarge the space for amplitude and frequency control of coexisting attractors, the constants for offset boosting are modified accordingly. When $a = 0.4$ and $b = 1$, $G(y) = |y| - 20$, $F(z) = |z| - 20$, parameter c varies in $[0.8, 2]$, system CSLECS2 exhibits coexisting chaos of conditional symmetry with rescaled amplitude and frequency, as shown in Fig. 11.

4. Circuit Implementation

In the following, based on PSpice software, circuit implementations are used to prove the coexisting oscillations of conditional symmetry. By constructing various modules for integration, absolute value function operation, and phase reversal, two circuits are designed for reproducing the coexisting hidden attractors, where the operational amplifier OPA404, ideal multiplier, diode D1N4500 are applied for signal calculation.

For saturation of the operational amplifier, all the variables in system CSNECS6 are rescaled by a factor of ten. Thus system CSNECS6 becomes

$$\begin{cases} \dot{x} = y, \\ \dot{y} = |z| - 3, \\ \dot{z} = 10x^2 - 10y^2 + 10xy + 4x|z| - 12x + 0.1a. \end{cases} \tag{2}$$

The corresponding circuit equation is

$$\begin{cases} \dot{x} = \dfrac{1}{R_1C_1}y, \\ \dot{y} = \dfrac{1}{R_2C_2}|z| - \dfrac{3}{R_3C_2}, \\ \dot{z} = \dfrac{10}{R_4C_3}x^2 - \dfrac{10}{R_5C_3}y^2 + \dfrac{10}{R_6C_3}xy \\ \qquad + \dfrac{4}{R_7C_3}x|z| - \dfrac{12}{R_8C_3}x + \dfrac{0.1a}{R_9C_3}. \end{cases} \tag{3}$$

Here $a = 1$, and the corresponding circuit parameters are $C_1 = C_2 = C_3 = 1\,\text{nF}$, $R_4 = R_5 = R_6 = 10\,\text{k}\Omega$, $R_7 = 25\,\text{k}\Omega$, $R_8 = 8.4\,\text{k}\Omega$, $R_9 = 1000\,\text{k}\Omega$, $R_1 = R_2 = R_3 = R_{11} = R_{12} = R_{13} = R_{14} = R_{15} = R_{16} = R_{17} = R_{18} = R_{19} = R_{20} = 100\,\text{k}\Omega$. The circuit schematic is shown in Fig. 12, where V represents $|z|$. The circuit gives coexisting oscillations as shown in Figs. 14(a) and 14(b).

The system CSLECS3 can be transformed into the following circuit equation which corresponds to the circuit shown in Fig. 13,

$$\begin{cases} \dot{x} = \dfrac{1}{R_1C_1}y, \\ \dot{y} = \dfrac{c}{R_2C_2}|yz| - \dfrac{4c|y|}{R_3C_2} + \dfrac{0.1}{R_4C_2}y|y| - \dfrac{1}{R_5C_2}x, \\ \dot{z} = \dfrac{0.5}{R_6C_3}x^2 - \dfrac{a}{R_7C_3}xy - \dfrac{b}{R_8C_3}x|z| + \dfrac{4b}{R_9C_3}x. \end{cases} \tag{4}$$

Here $a = 0.8$, $b = 0.5$, $c = 0.5$, and the corresponding circuit parameters are $C_1 = C_2 = C_3 = 1\,\text{nF}$,

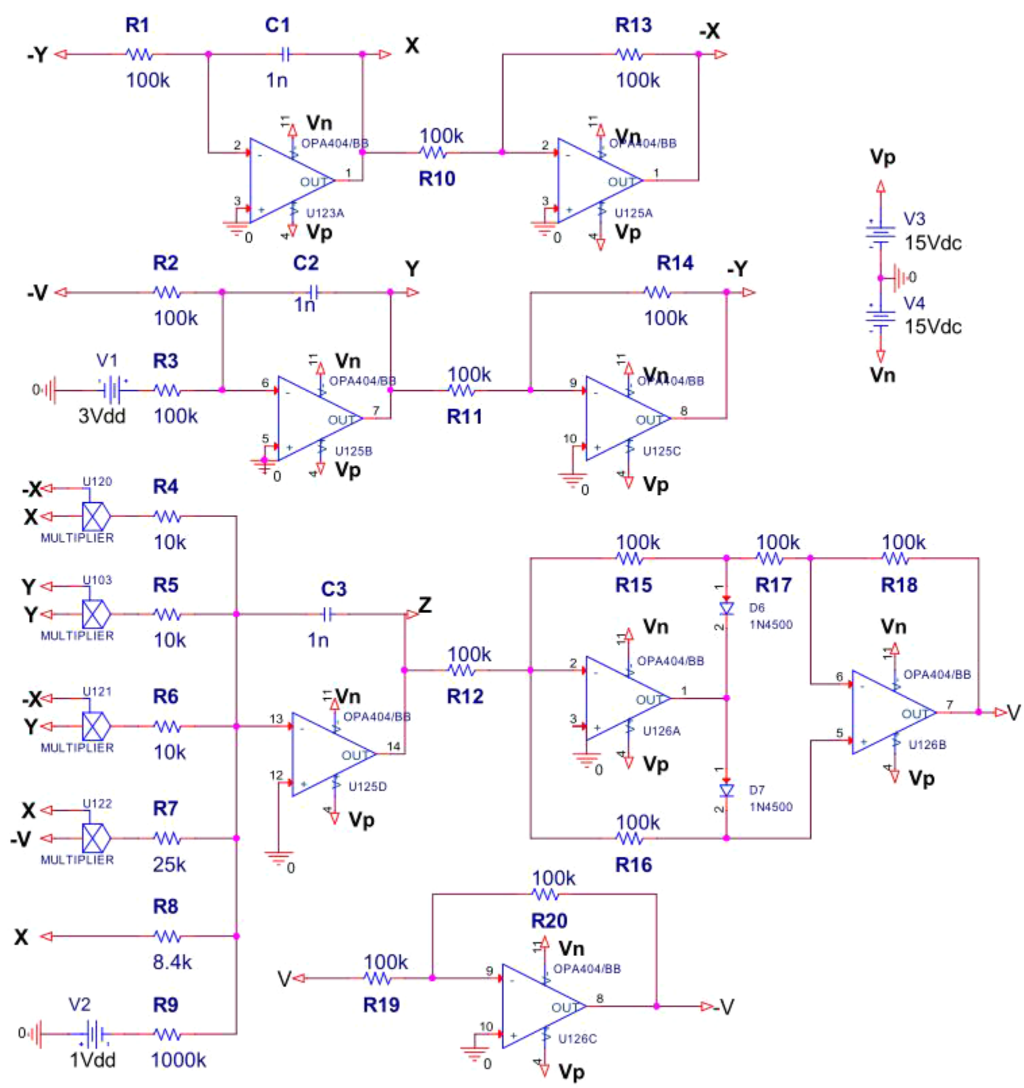

Fig. 12. Circuit schematic of system CSNECS6.

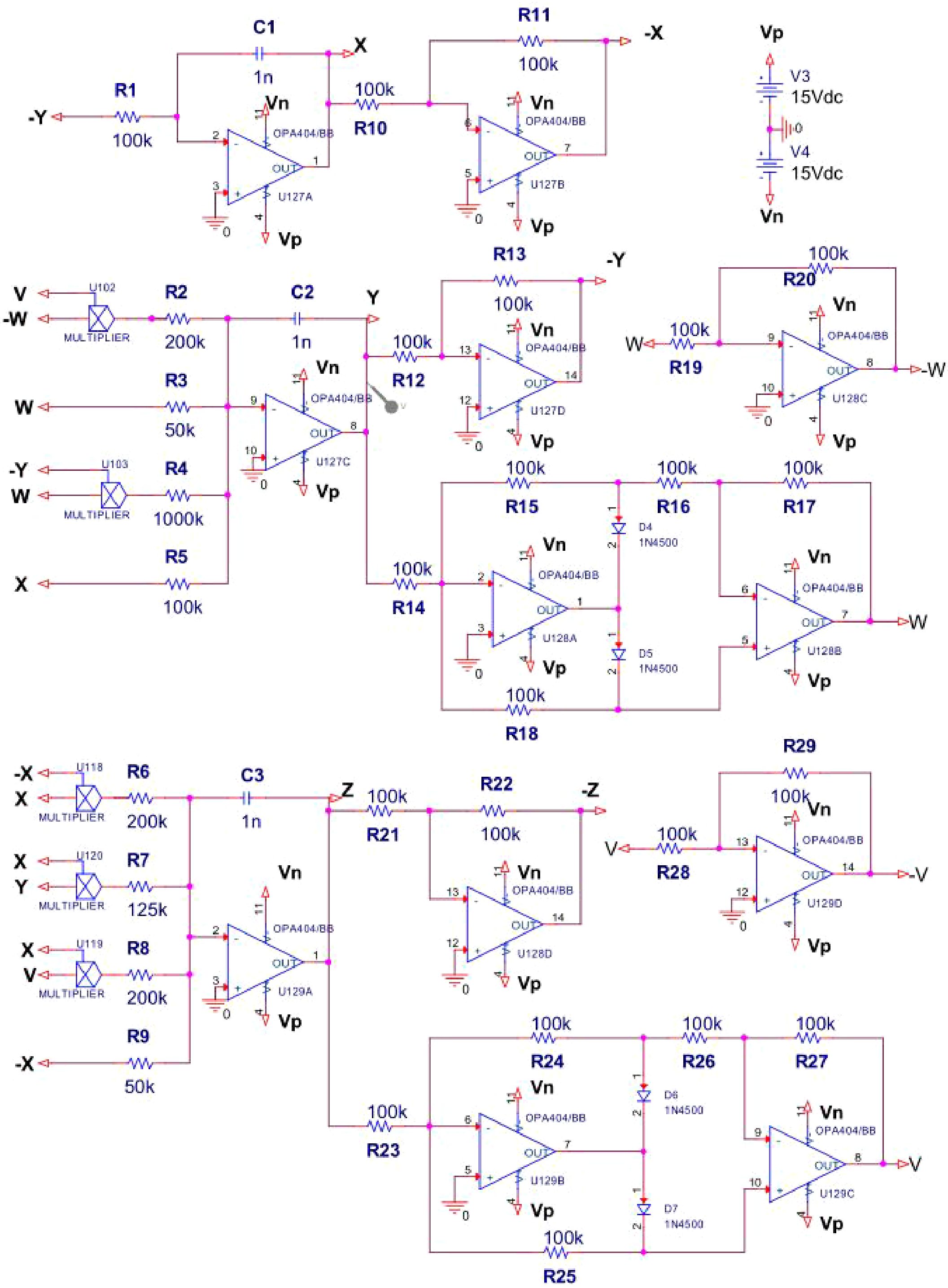

Fig. 13. Circuit schematic of system CSLECS3.

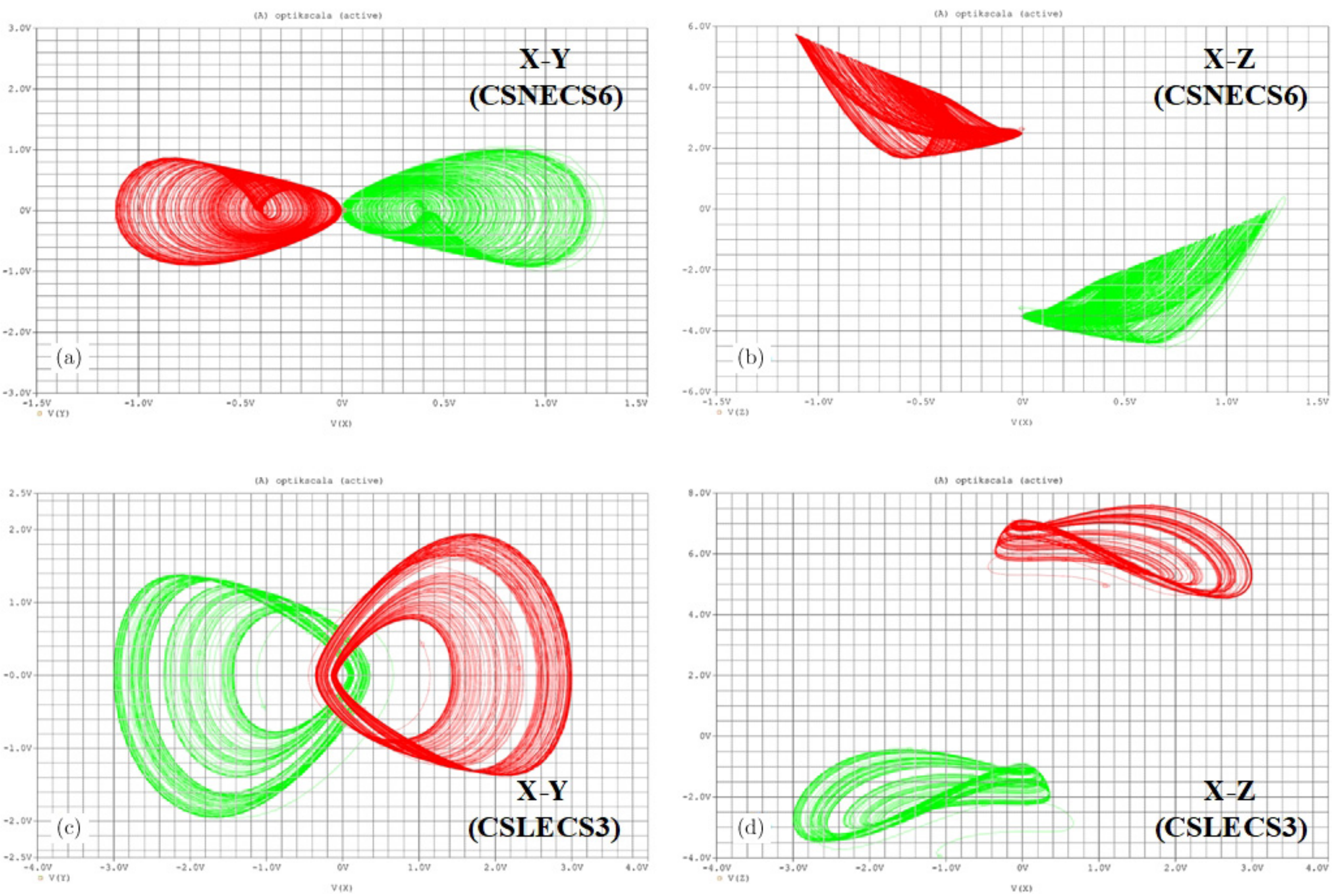

Fig. 14. Coexisting attractors shown in the oscilloscope obtained from PSpice.

$R_2 = R_6 = R_8 = 200\,\text{k}\Omega$, $R_3 = R_9 = 50\,\text{k}\Omega$, $R_4 = 1000\,\text{k}\Omega$, $R_7 = 125\,\text{k}\Omega$, $R_1 = R_5 = R_{10} = R_{11} = R_{12} = R_{13} = R_{14} = R_{15} = R_{16} = R_{17} = R_{18} = R_{19} = R_{20} = R_{21} = R_{22} = R_{23} = R_{24} = R_{25} = R_{26} = R_{27} = R_{28} = R_{29} = 100\,\text{k}\Omega$. W and V in the circuit represent the quantities $|y|$ and $|z|$. The corresponding circuit for system CSLECS3 gives coexisting oscillations as shown in Figs. 14(c) and 14(d).

5. Conclusion and Discussion

Offset-boosting-induced polarity recovery also exists in asymmetric systems with no equilibrium or with lines of equilibria. Such new examples are obtained when those systems are modified with a piecewise absolute value function for polarity balance. Like other cases, coexisting oscillations are found as predicted. This result enriches the gallery of hidden attractors and those chaotic systems of conditional symmetry. Furthermore, some other cases [Jahanshahi *et al.*, 2019; Ren *et al.*, 2018; Vo *et al.*, 2019; Lin & Wang, 2020] could be checked for their conditional symmetric versions. For example, applying the same approach to the system in the first hyperjerk system with no equilibrium [Ren *et al.*, 2018], conditional rotational symmetry can be constructed based on polarity reversal of x, y and offset boosting of z. In fact, as predicted, offset-boosting-based polarity balance exists in many dynamical systems, which provides a new scheme for producing coexisting chaotic oscillations. In this case, chaotic signals of either desired polarity can be conveniently obtained.

Acknowledgments

This work was supported by the National Nature Science Foundation of China (Grant Nos. 61871230 and 61971228), the Natural Science Foundation of Jiangsu Province (Grant No. BK20181410), and a Project Funded by the Priority Academic Program Development of Jiangsu Higher Education Institutions (PAPD).

References

Bao, B., Xu, Q., Bao, H. & Chen, M. [2016] "Extreme multistability in a memristive circuit," *Electron. Lett.* **52**, 1008–1010.

Bao, B., Bao, H., Wang, N., Chen, M. & Xu, Q. [2017a] "Hidden extreme multistability in memristive hyperchaotic system," *Chaos Solit. Fract.* **94**, 102–111.

Bao, H., Wang, N., Bao, B., Chen, M. & Wang, G. [2017b] "Initial condition-dependent dynamics and transient period in memristor-based hypogenetic jerk system with four line equilibria," *Commun. Nonlin. Sci. Numer. Simul.* **57**, 264–275.

Bayani, A., Rajagopal, K., Khalaf, A. J. M., Jafari, S., Leutcho, G. D. & Kengne, J. [2019] "Dynamical analysis of a new multistable chaotic system with hidden attractor: Antimonotonicity, coexisting multiple attractors, and offset boosting," *Phys. Lett. A* **383**, 1450–1456.

Çavuşoğlu, Ü., Panahi, S., Akgül, A., Jafari, S. & Sezgin, K. [2019] "A new chaotic system with hidden attractor and its engineering applications: Analog circuit realization and image encryption," *Analog Integr. Circuits Syst.* **98**, 85–99.

Jafari, S. & Sprott, J. C. [2013a] "Simple chaotic flows with a line equilibrium," *Chaos Solit. Fract.* **57**, 79–84.

Jafari, S. & Sprott, J. C. [2013b] "Elementary quadratic chaotic flows with no equilibria," *Phys. Lett. A* **377**, 699–702.

Jafari, S., Sprott, J. C. & Molaie, M. [2016] "A simple chaotic flow with a plane of equilibria," *Int. J. Bifurcation and Chaos* **26**, 1650098-1–6.

Jahanshahi, H., Shahriari-Kahkeshi, M., Alcaraz, R., Wang, X., Singh, V. P. & Pham, V. T. [2019] "Entropy analysis and neural network-based adaptive control of a non-equilibrium four-dimensional chaotic system with hidden attractors," *Entropy* **21**, 156.

Jesus, M. P., Ernesto, Z. S., Christos, V., Jafari, S., Jacques, K. & Rajagopal, K. [2018] "A new fractional-order chaotic system with different families of hidden and self-excited attractors," *Entropy* **20**, 564.

Kuznetsov, N. V., Leonov, G. A., Mokaev, T. N., Prasad, A. & Shrimali, M. D. [2018] "Finite-time Lyapunov dimension and hidden attractor of the Rabinovich system," *Nonlin. Dyn.* **92**, 267–285.

Kuznetsov, N. V. & Mokaev, T. N. [2019] "Numerical analysis of dynamical systems: Unstable periodic orbits, hidden transient chaotic sets, hidden attractors, and finite-time Lyapunov dimension," *J. Phys.: Conf. Ser.* **1205**, 012034.

Leonov, G. A., Vagaitsev, V. I. & Kuznetsov, N. V. [2011] "Localization of hidden Chua's attractors," *Phys. Lett. A* **375**, 2230–2233.

Leonov, G. A., Vagaitsev, V. I. & Kuznetsov, N. V. [2012] "Hidden attractor in smooth Chua systems," *Physica D* **241**, 1482.

Leonov, G. A. & Kuznetsov, N. V. [2013] "Hidden attractors in dynamical systems from hidden oscillations in Hilbert–Kolmogov, Aizerman, and Kalman problems to hidden chaotic attractors in Chua circuits," *Int. J. Bifurcation and Chaos* **23**, 1330002-1–69.

Leonov, G. A., Vagaitsev, V. I. & Kuznetsov, N. V. [2015] "Homoclinic orbits, and self-excited and hidden attractors in a Lorenz-like system describing convective fluid motion," *Eur. Phys. J. Spec. Top.* **224**, 1421–1458.

Li, C. & Sprott, J. C. [2014a] "Coexisting hidden attractors in a 4-D simplified Lorenz system," *Int. J. Bifurcation and Chaos* **24**, 1450034-1–12.

Li, C. & Sprott, J. C. [2014b] "Chaotic flows with a single nonquadratic term," *Phys. Lett. A* **378**, 178–183.

Li, C., Sprott, J. C. & Thio, W. [2014] "Bistability in a hyperchaotic system with a line equilibrium," *J. Exp. Theor. Phys.* **118**, 494–500.

Li, C., Hu, W., Sprott, J. C. & Wang, X. [2015a] "Multistability in symmetric chaotic systems," *Eur. Phys. J. Spec. Top.* **224**, 1493–1506.

Li, C., Pehlivan, I. & Sprott, J. C. [2015b] "A novel four-wing strange attractor born in bistability," *IEICE Electron. Expr.* **12**, 20141116.

Li, C., Sprott, J. C. & Thio, W. [2015c] "Linearization of the Lorenz system," *Phys. Lett. A* **379**, 888–893.

Li, C., Sprott, J. C. & Xing, H. [2016a] "Hypogenetic chaotic jerk flows," *Phys. Lett. A* **380**, 1172–1177.

Li, P., Zheng, T. & Li, C. [2016b] "A unique jerk system with hidden chaotic oscillation," *Nonlin. Dyn.* **86**, 197–203.

Li, C. & Sprott, J. C. [2017] "How to bridge attractors and repellors," *Int. J. Bifurcation and Chaos* **27**, 1750149-1–11.

Li, C., Sprott, J. C. & Xing, H. [2017] "Constructing chaotic systems with conditional symmetry," *Nonlin. Dyn.* **87**, 1351–1358.

Li, C., Sprott, J. C., Liu, Y., Gu, Z. & Zhang, J. [2018] "Offset boosting for breeding conditional symmetry," *Int. J. Bifurcation and Chaos* **28**, 1850163-1–13.

Li, C., Xu, Y., Chen, G., Liu, Y. & Zhang, J. [2019] "Conditional symmetry: Bond for attractor growing," *Nonlin. Dyn.* **95**, 1245–1256.

Lin, H. & Wang, C. [2020] "Influences of electromagnetic radiation distribution on chaotic dynamics of a neural network," *Appl. Math. Comput.* **369**, 124840.

Molaie, M., Jafari, S. & Sprott, J. C. [2013] "Simple chaotic flows with one stable equilibrium," *Int. J. Bifurcation and Chaos* **23**, 1350188-1–7.

Nazarimehr, F., Rajagopal, K., Kengne, J., Jafari, S. & Pham, V. T. [2018] "A new four-dimensional system containing chaotic or hyper-chaotic attractors with no equilibrium, a line of equilibria and unstable equilibria," *Chaos Solit. Fract.* **111**, 108–118.

Pham, V. T., Volos, C., Vaidyanathan, S., Le, T. & Vu, V. [2015] "A memristor-based hyperchaotic system with hidden attractors: Dynamics, synchronization and circuital emulating," *J. Eng. Sci. Technol. Rev.* **8**, 205–214.

Pham, V. T., Volos, C., Jafari, S. & Kapitaniak, T. [2017] "A novel cubic-equilibrium chaotic system with coexisting hidden attractors: Analysis, and circuit implementation," *J. Circuit. Syst. Comp.* **27**, 1850066.

Pham, V. T., Volos, C., Kingni, S. T., Kapitaniak, T. & Jafari, S. [2018] "Bistable hidden attractors in a novel chaotic system with hyperbolic sine equilibrium," *Circ. Syst. Sign. Process.* **37**, 1028–1043.

Ren, S. L., Panahi, S., Rajagopal, K., Akgül, A., Pham, V. T. & Jafari, S. [2018] "A new chaotic flow with hidden attractor: The first hyperjerk system with no equilibrium," *Z. Naturforsch. A* **73**, 239–249.

Sprott, J. C. [2014] "Simplest chaotic flows with involutional symmetries," *Int. J. Bifurcation and Chaos* **24**, 1450009-1–9.

Sprott, J. C. [2015] "Strange attractors with various equilibrium types," *Eur. Phys. J. Spec. Top.* **224**, 1409–1419.

Tang, Y. X., Khalaf, A. J. M., Rajagopal, K., Pham, V. T., Jafari, S. & Tian, Y. [2018] "A new nonlinear oscillator with infinite number of coexisting hidden and self-excited attractors," *Chinese Phys. B* **27**, 040502.

Vo, T. P., Shaverdi, Y., Khalaf, A. J. M., Alsaadi, F. E., Hayat, T. & Pham, V. T. [2019] "A giga-stable oscillator with hidden and self-excited attractors: A megastable oscillator forced by his twin," *Entropy* **21**, 535.

Wang, X. & Chen, G. [2012] "A chaotic system with only one stable equilibrium," *Commun. Nonlin. Sci. Numer. Simul.* **17**, 1264–1272.

Wang, Y., Sun, K., He, S. & Wang, H. [2014] "Dynamics of fractional-order sinusoidally forced simplified Lorenz system and its synchronization," *Eur. Phys. J. Spec. Top.* **223**, 1591–1600.

Wei, Z., Yu, P., Zhang, W. & Yao, M. [2015] "Study of hidden attractors, multiple limit cycles from Hopf bifurcation and boundedness of motion in the generalized hyperchaotic Rabinovich system," *Nonlin. Dyn.* **82**, 131–141.

Wolf, A., Swift, J. B., Swinney, H. L. & Vastano, J. A. [1985] "Determining Lyapunov exponents from a time series," *Physica D* **16**, 285–317.

Yang, Q., Wei, Z. & Chen, G. [2010] "An unusual 3D autonomous quadratic chaotic system with two stable node-foci," *Int. J. Bifurcation and Chaos* **20**, 1061–1083.

Zhang, X. & Wang, C. [2019] "Multiscroll hyperchaotic system with hidden attractors and its circuit implementation," *Int. J. Bifurcation and Chaos* **29**, 1950117-1–14.

Zhou, L., Wang, C. & Zhou, L. [2018a] "A novel no-equilibrium hyperchaotic multi-wing system via introducing memristor," *Int. J. Circ. Theor. Appl.* **46**, 84–98.

Zhou, L., Wang, C., Zhang, X. & Yao, W. [2018b] "Various attractors, coexisting attractors and antimonotonicity in a simple fourth-order memristive twin-T oscillator," *Int. J. Bifurcation and Chaos* **28**, 1850050-1–18.